# Benzenediazonium Ion. Generality, Consistency, and Preferability of the Electron Density Based Dative Bonding Model

Rainer Glaser* and Christopher J. Horan[1]

*Department of Chemistry, University of Missouri–Columbia, Columbia, Missouri 65211*

*Received August 16, 1995*[⊗]

The potential energy surface of benzenediazonium ion **1** has been examined with RHF, DFT, and MP2 theory, and energies also were determined up to the level QCISD(T)//MP2. The previously accepted potential energy surface characteristics are revised. The nature of the C–N bonding in **1** was studied to establish the generality of the electron density based dative bonding model for diazonium ions, to test its consistency with experimental properties, and to argue for its preferability over purely formal bonding models. The analyses show that for **1**, as for aliphatic diazonium ions, it is the hydrocarbon fragment and not the $N_2$ group that carries most of the positive charge. Compelling evidence is provided for the synergistic interplay between $\sigma$-dative C←$N_2$ and $\pi$-back-dative C→$N_2$ bonding. The analysis of the noble gas systems Ph–$E^+$ (E = He, Ne, Ar) corroborates the importance of the internal polarization within $N_2$ and of the lone pair hybridization for dative bond formation. Experimental properties of **1** including its structural characteristics, the diazonio function's substituent constant and the opposing sign dual substituent parameter reaction constants for dediazoniations and automerizations, its reactivities toward nucleophiles and electrophiles, and its $^{13}C$ and $^{15}N$ NMR chemical shifts show no conflict but are fully compatible with the dative bonding model. The dative bond descriptions $R^+$←N≡N or $R^+$⇄N≡N are clearly preferable over the commonly used Lewis–Kekulé structures because they represent more closely the actual electron density distribution.

## Introduction

We have been interested in two types of deamination reactions and their relation to modifications of nucleic acids. The first of these relates to the deamination of aliphatic and aromatic amines and their role in the alkylation or arylation of DNA.[2] The other relates to the deamination of the amino groups of the DNA bases in nucleic acids.[3] Both of these deamination processes have important consequences for DNA, and their mechanisms are not well understood. Aromatic diazonium ions are important in both of these instances. Arenediazonium ions are implicated in DNA arylations which may proceed via the phenyl cation[4] or radical.[5] The study of benzenediazonium ion also is central to the understanding of the heteroaromatic diazonium ions derived from DNA base deamination.[3]

In this context, we have been studying diazonium ions with physical and theoretical organic methods. On the basis of topological electron density analyses, we proposed a new bonding model for diazonium ions.[6a–c] This bonding model emphasizes dative bonding between an overall essentially neutral $N_2$ group and the positively charged hydrocarbon fragment. Only in heterosubstituted diazonium ions[7] and in complexes formed between $N_2^+$ and some noble gases[8] is the charge actually associated with the diazo group. The significance of any bonding model is decided by its ability to explain experimental observations consistently and better than alternative models. Thus, we provided direct experimental support for this density-based bonding model via the analyses of the first crystal structures of *aliphatic* diazonium ions,[9] and studies of the "incipient nucleophilic attack" established a further link to experiment.[10]

The purpose of the present paper is 4-fold. First, we show that the bonding model is general as it applies not only to the previously studied aliphatic systems but also to the parent aromatic system, the benzenediazonium ion **1**. Second, we discuss the noble gas systems [Ph–E]$^+$ (E = He, Ne, Ar) in comparison to **1** to assess the importance of internal $N_2$ polarization to the binding in

Downloaded via UNIV OF MISSOURI COLUMBIA on September 10, 2022 at 14:26:39 (UTC).
See https://pubs.acs.org/sharingguidelines for options on how to legitimately share published articles.

[⊗] Abstract published in *Advance ACS Abstracts,* November 1, 1995.

(1) (a) Part of the projected Ph.D. Dissertation of C.J.H., University of Missouri–Columbia, 1995. (b) Presented in part at the 208th National Meeting of the American Chemical Society, Washington, DC, Aug 1994, at the Midwest Regional American Chemical Society Meeting, Columbia, MO, Nov 1993, and at the XIIth International Conference on Phosphorus Chemistry, Toulouse, France, July 1992.

(2) (a) *DNA Methylation and Gene Regulation*; Holliday, R., Monk, M., Pugh, J. E., Eds.; The Royal Society: London, 1990. (b) Excellent reviews can be found in Chapters 12–14 of *Chemical Carcinogens*, Vol. 2; Searle, Ch. E., Ed.; American Chemical Society: Washington, DC, 1984; ACS Monograph Series 182. (c) Chin, A.; Hung, M.-H.; Stock, L. M. *J. Org. Chem.* **1981**, *46*, 2203. (d) Hung, M.-H.; Stock, L. M. *J. Org. Chem.* **1982**, *47*, 448.

(3) Tannenbaum, S. R.; Tamir, S.; Rojas-Walker, T. D.; Wishnok, J. S. *Nitrosamines and Related N-Nitroso Compounds–Chemistry and Biochemistry*; Loeppky, R. N., Michejda, C. J., Eds.; American Chemical Society: Washington, DC, 1994; ACS Symposium Series 553, Chapter 10, pp 120–135.

(4) Behr, J. P. *J. Chem. Soc., Chem. Commun.* **1989**, 101.

(5) (a) Griffiths, J.; Murphy, J. A. *J. Chem. Soc., Chem. Commun.* **1992**, 24. (b) Arya, D. P.; Warner, P. M.; Jebaratnam, D. J. *Tetrahedron Lett.* **1993**, *34*, 7823.

(6) (a) Glaser, R. *J. Phys. Chem.* **1989**, *93*, 7993. (b) Glaser, R.; Choy, G. S.-C.; Hall, M. K. *J. Am. Chem. Soc.* **1991**, *113*, 1109. (c) Glaser, R. *J. Comput. Chem.* **1990**, *11*, 663. (d) Glaser, R.; Horan, C. J.; Choy, G. S.-C.; Harris, B. L. *Phosphorus, Sulfur Silicon* **1993**, *77*, 73. (e) Horan, C. J.; Glaser, R. *J. Phys. Chem.* **1994**, *98*, 3989.

(7) (a) Glaser, R.; Choy, G. S.-C. *J. Phys. Chem.* **1991**, *95*, 7682. (b) Glaser, R.; Choy, G. S.-C.; Horan, C. J. *J. Org. Chem.* **1992**, *57*, 995. (c) Glaser, R.; Choy, G. S.-C. *J. Org. Chem.* **1992**, *57*, 4976. (d) Glaser, R.; Choy, G. S.-C. *J. Am. Chem. Soc.* **1993**, *115*, 2340. (e) Christe, K. O.; Wilson, W. W.; Dixon, D. A.; Khan, S. I.; Bau, R.; Metzenthin, T.; Lu, R. *J. Am. Chem. Soc.* **1993**, *115*, 1836.

(8) Bieske, E. J.; Maier, J. P. *Chem. Rev.* **1993**, *93*, 2603.

(9) (a) Glaser, R.; Chen, G. S.; Barnes, C. L. *Angew. Chem., Int. Ed. Engl.* **1992**, *31*, 740. (b) Chen, G. S.; Glaser, R.; Barnes, C. L. *J. Chem. Soc., Chem. Commun.* **1993**, 1530.

(10) (a) Glaser, R.; Horan, C. J.; Nelson, E.; Hall, M. K. *J. Org. Chem.* **1992**, *57*, 215. (b) Horan, C. J.; Barnes, C. L.; Glaser, R. *Acta Crystallogr.* **1993**, *C49*, 507. (c) Horan, C. J.; Haney, P. E.; Barnes, C. L.; Glaser, R. *Acta Crystallogr.* **1993**, *C49*, 1525. (d) Horan, C. J.; Barnes, C. L.; Glaser, R. *Chem. Ber.* **1993**, *126*, 243. (e) Glaser, R.; Mummert, C. L.; Horan, C. J.; Barnes, C. L. *J. Phys. Org. Chem.* **1993**, *6*, 201. (f) Glaser, R.; Horan, C. *Can. J. Chem.*, submitted.

0022-3263/95/1960-7518$09.00/0 © 1995 American Chemical Society

**Table 1. Binding and Relative Energies**

| parameter | 1a | 1b | 1c | 1d | 1e | 1a vs 1b | 1a vs 1c | 1a vs 1d | 1a vs 1e |
|---|---|---|---|---|---|---|---|---|---|
| $E$,[a] RHF/6-31G* | 25.61 | 0.53 | 0.22 | | | 25.08 | 25.39 | | |
| ΔVZPE,[b-d] RHF/6-31G* | −4.64 | −0.23 | −0.18 | | | −4.89 | −4.95 | | |
| $E$, MP2(fc)/6-31G*//A | 37.24 | 1.80 | 1.34 | | | 35.44 | 35.89 | | |
| $E$, MP3(fc)/6-31G*//A | 33.70 | 1.39 | 1.01 | | | 32.31 | 32.69 | | |
| $E$, MP2(fu)/6-31G* | 38.64 | 2.43 | 2.16 | −0.42 | −2.56 | 36.21 | 36.48 | 39.06 | 41.20 |
| ΔVZPE, MP2(fu)/6-31G* | −5.56 | −0.48 | −0.55 | −4.37 | −2.62 | −5.08 | −5.01 | −1.19 | −2.94 |
| $E$, MP2(fc)/6-31G*//B[e] | 37.93 | 2.30 | 2.04 | −0.81 | −2.86 | 35.63 | 35.89 | 38.74 | 40.79 |
| $E$, MP3(fc)/6-31G*//B | 33.43 | 1.60 | 1.39 | −2.16 | −4.38 | 31.83 | 32.04 | 35.59 | 37.81 |
| $E$, MP4(sdtq,fc)/6-31G*//B | 34.28 | 2.16 | 1.80 | −3.38 | −4.56 | 32.11 | 32.48 | 37.66 | 38.84 |
| $E$, QCISD(T,fc)/6-31G*//B | 32.20 | 1.99 | 1.65 | −4.35 | −5.33 | 30.21 | 30.55 | 36.55 | 37.53 |
| $E$, Becke3LYP/6-31G* | 37.74 | 1.28 | 1.17 | 1.43 | −2.10 | 36.46 | 36.57 | 36.31 | 39.84 |
| ΔVZPE, Becke3LYP/6-31G* | −5.44 | −0.38 | −0.47 | −4.12 | −2.08 | −5.06 | −4.97 | −1.32 | −3.36 |

[a] $E$ represents binding energies for **1a**, **1b**, **1c**, **1d**, and **1e**. The reaction energies for $RNN^+ \rightarrow R^+ + NN$ in kilocalories per mole. For **1a** vs **1b**, **1a** vs **1c**, **1a** vs **1d**, and **1a** vs **1e**, $E$ represents relative energies. [b] ΔVZPE in kilocalories per mole and scaled by factor 0.9. Addition of the ΔVZPE values to $E_b$ or $E_{rel}$ gives the respective VZPE corrected values. [c] ΔVZPE = VZPE($Ph^+$) + VZPE(NN) − VZPE($PhNN^+$). [d] ΔVZPE = VZPE(M) − VZPE(**1a**) with M = **1b**, **1c**, **1d**, and **1e**. [e] A represents the RHF/6-31G* geometry and B represents the MP2(fu)/6-31G* geometry.

diazonium ions. Third, this study of **1** allows for a much broader examination of the consistency of the bonding model with a variety of experimental data because aromatic diazonium ions are experimentally more accessible. With the generality established and its consistency tested, we will then argue for the preferability of the dative bonding model over purely formal descriptions of C−N bonding. The results of our study should also be of more general interest since aromatic diazonium ions are important for the synthesis of azo dyes[11] and as probes in the studies of colloids[12] and they find broad utility as aryl radical sources for synthetic precursors.[13-15] The Sandmeyer and Schiemann reactions are both important syntheses for halogenated aromatic compounds.[16] Diazonium ions are central to the Gomberg−Bachmann coupling reaction and the intramolecular Pschorr reaction.[17]

## Theoretical Methods

Ab initio calculations were carried out with Gaussian92/DFT[18,19] and earlier versions on IBM RS-6000 Models 560, 580, and 590 and Silicon Graphics Indigo workstations. Geometries were optimized within the symmetry constraints specified, and harmonic vibrational frequencies were determined analytically for the stationary structures. The optimization and the vibrational analyses were carried out at the RHF/6-31G* level, with the inclusion of dynamic electron correlation at the MP2-(full)/6-31G* level, as well as with density functional theory[20] using the hybrid method Becke3LYP[21] in conjunction with the 6-31G* basis set. For the calculation of relative and binding energies computed at the RHF level, differences in vibrational zero-point energies (ΔVZPE) were scaled (factor 0.9). The vibrational zero-point energies determined at the MP2 level and with the semiempirical DFT method[22] are known to be more accurate and were used unscaled. Aside from the energies determined at the RHF, MP2, and DFT levels used for the potential energy exploration, we also determined two additional sets of more reliable energies. The first of these is based on the RHF/6-31G* structures and involves the calculation of energies up to the third order of Møller−Plesset perturbation theory in the frozen core approximation with the 6-31G* basis set. Our best energies were determined at the QCISD(T,fc) level[23] using the 6-31G* basis set and with the MP2(full)/6-31G* geometries. Binding and relative energies are collected in Table 1 and geometries are shown in Figure 1. Electronic structures were examined at the levels RHF/6-31G* and MP2(full)/6-31G*. Topological and integrated properties were determined with the programs Extreme and Proaim.[24] Graphical representations of the first atomic moments were evaluated with the program Dipoles.[25] NMR chemical shifts for **1a** were determined with the IGLO method at the "Double Zeta" and "Basis II" levels[26] using the RHF/6-31G* geometry. Basis II closely resembles the 6-31G* basis set used in the topological analysis.

(11) For previous papers on examples of diazo coupling, see: (a) Zollinger, H. *Melliand Textilber.* **1988**, *69*, 644. (b) Skrabal, P.; Zollinger, H. *Dyes Pigm.* **1988**, *9*, 201. (c) Koller, S.: Zollinger, H. *Helv. Chim. Acta* **1970**, *53*, 78. (d) Szele, I.; Zollinger, H. *Top. Curr. Chem.* **1983**, *112*, 1. (e) Zollinger, H. *Color Chemistry. Syntheses, Properties and Applications of Organic Dyes and Pigments*, 2nd ed.; VCH: Weinheim, 1991.

(12) (a) Chaudhuri, A.; Loughlin, J. A.; Romsted, L. S.; Yao, J. *J. Am. Chem. Soc.* **1993**, *115*, 8351. (b) Chaudhuri, A.; Romsted, L. S.; Yao, J. *J. Am. Chem. Soc.* **1993**, *115*, 8362.

(13) *The Chemistry of Diazonium and Diazo Groups*; Patai, S., Ed.; John Wiley & Sons: New York, 1978.

(14) Lloris, M. E.; Abramovitch, R. A.; Marquet, J.; Moreno-Manas, M. *Tetrahedron* **1992**, *48*, 6909.

(15) Zollinger, H. *Diazo Chemistry I*; VCH Publishers: New York, 1994.

(16) For examples of each, see: (a) Clarke, H. T.; Read, R. R. *Org. Synth.* **1941**, *1*, 514. (b) Suschitsky, H. *Adv. Fluorine Chem.* **1965**, *4*, 1.

(17) For a review, see: Abramovitch, R. A. *Adv. Free-Radical Chem.* **1966**, *2*, 87.

(18) Gaussian92/DFT, Revision G.2: Frisch, M. J.; Trucks, G. W.; Schlegel, H. B.; Gill, P. M.; Johnson, B. G.; Wong, M. W.; Foresman, J. B.; Robb, M. A.; Head-Gordon, M.; Replogle, E. S.; Gomperts, R.; Andres, J. L.; Raghavachari, K.; Binkley, J. S.; Gonzalez, C.; Martin, R. L.; Fox, D. J.; Defrees, D. J.; Baker, J.; Stewart, J. J. P.; Pople, J. A., Gaussian Inc., Pittsburgh, PA, 1993, and earlier versions.

(19) Hehre, W. J.; Radom, L.; Schleyer, P. v. R.; Pople, J. A. *Ab Initio Molecular Orbital Theory*; John Wiley & Sons: New York, 1986.

(20) (a) March, N. H. *Electron Density Theory of Atoms and Molecules*; Academic Press, Inc., San Diego, CA, 1992. (b) Labanowski, J. K.; Andzelm, J. W.; Eds. *Density Functional Methods in Chemistry*; Springer-Verlag; New York, 1991. (c) Parr, R. G.; Yang W. *Functional Theory of Atoms and Molecules*; Oxford University Press: New York, 1989.

(21) Becke3LYP: (a) Becke, A. D. *Phys. Rev. A* **1986**, *33*, 2786. (b) Becke, A. D. *J. Chem. Phys.* **1988**, *88*, 2547. (c) Lee, C.; Yang, W.; Parr, R. G. *Phys. Rev. B* **1988**, *37*, 785.

(22) See, for example: Stephens, P. J.; Devlin, F. J.; Chabalowski, C. F.; Frisch, M. J. *J. Phys. Chem.* **1994**, *98*, 11623.

(23) Pople, J. A.; Head-Gordon, M; Raghavachari, K. *J. Phys. Chem.* **1987**, *87*, 5968.

(24) (a) Biegler-König, F. W.; Bader, R. F. W.; Tang, T.-H. *J. Comput. Chem.* **1982**, *3*, 317. (b) Bader, R. F. W. *Atoms in Molecules—A Quantum Theory*; Clarendon Press: Oxford, U.K. 1990.

(25) Glaser, R., Department of Chemistry, University of Missouri—Columbia, 1990.

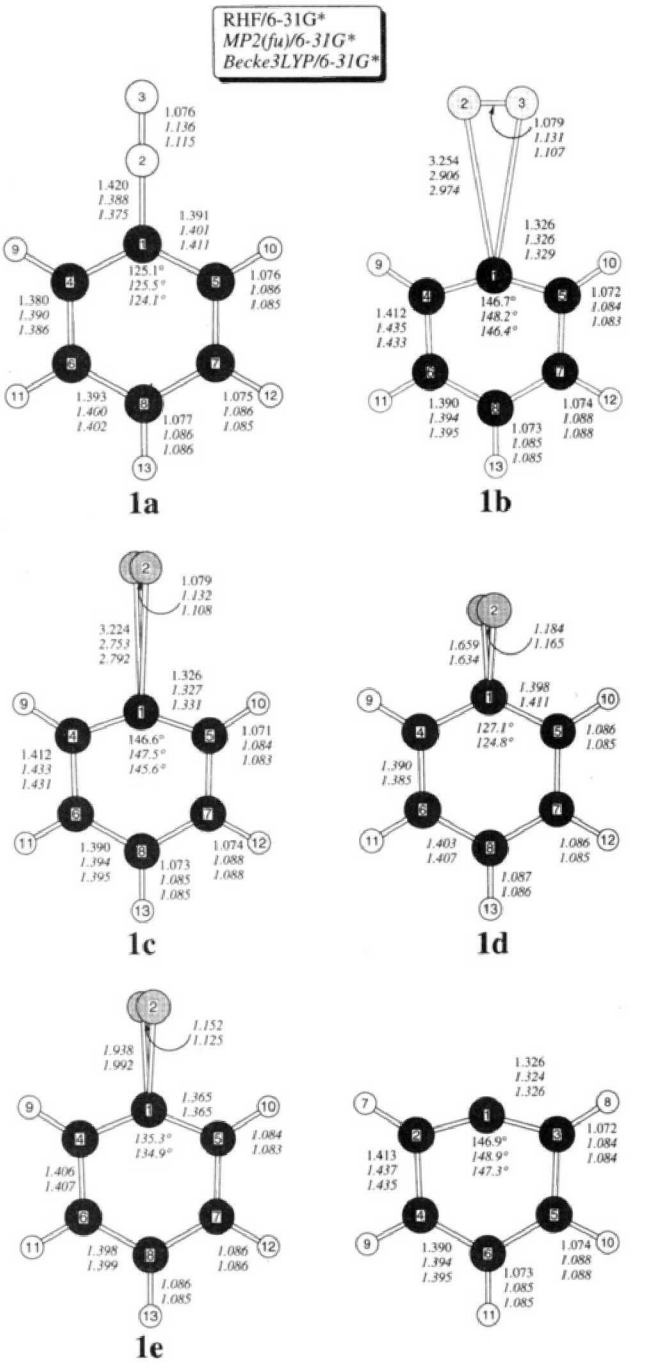


**Figure 1.** Molecular models of stationary structures of benzenediazonium ion (**1**) and phenyl cation.

## Results and Discussion

**Potential Energy Surface of Benzenediazonium Ion Revisited.** Minimal basis set calculations of **1** were reported by Dill, Schleyer, and Pople in their study of amino-substituted benzenediazonium ions[27] and by Alcock et al.[28] and Escudero et al.[29] in their studies of structures and charge distributions of *para*-substituted derivatives. A more detailed study of the RHF/STO-3G PES of **1** was reported by Vincent and Radom.[30] Their work suggested that, aside from the end-on $N_2$-coordinated structure, **1a**, a symmetric out-of-plane $N_2$-coordinated structure, **1c**, existed as a second minimum 34.3 kcal/mol higher in energy compared to that of **1a**. A partially optimized out-of-plane asymmetrically $\eta^2$-bridged structure was reported as the transition state structure for isomerization between **1a** and **1c** which was predicted to be significantly higher in energy (10.6 kcal/mol) compared to that of **1c**.

In the present work, we considered all of the stationary structures along the three cross sections of the potential energy hypersurface associated with the linear, the in-plane edge-on, and the out-of-plane edge-on approaches of $N_2$ to singlet phenyl cation (Figure 2, left). These cross sections were studied at the levels RHF/6-31G*, MP2-(full)/6-31G*, and DFT/6-31G*. The previously reported RHF-PES characteristics require revision, and our results suggest that the potential energy surface characteristics for edge-on coordinated structures are greatly affected by electron correlation. All of the energies discussed in the following refer to the QCISD(T,fc)/6-31G*//MP2(full)/6-31G* + ΔVZPE(MP2(full)/6-31G*) level unless noted otherwise. There is general agreement at all levels that the linear approach leads to a steady decrease in energy until the equilibrium structure **1a** (Figure 1) is reached. The structural data of **1a** are in excellent agreement with the available solid state structures of its salts[31] $PhN_2^+ X^-$ ($X^- = Cl^-, Br_3^-, BF_4^-$). There also is general agreement that the in-plane edge-on approach leads to only one stationary structure, **1b**, that this structure **1b** is only very weakly bonded compared to the free phenyl cation and $N_2$, and that the $N_2$ group is virtually completely disconnected with $C_{ipso}$–N distances greater than 2.7 Å. The vibrational analysis shows that **1b** is the transition state structure for automerization of **1a** with an activation energy of 25.1 kcal/mol.

Methodological differences do occur for the out-of-plane edge-on approach. The first difference relates to the characteristics of the RHF potential energy surface, and the other differences concern effects of electron correlation. At the RHF level, there exists only one stationary structure, **1c**. In contrast to the minimal basis set results, we find that this $C_{2v}$ symmetric out-of-plane structure is *not* a minimum but a second-order saddle point (Figure 1) and almost isoenergetic with the in-plane bridged transition state structure **1b**. The results suggest that the automerization of **1a** in the gas phase is a one-step process and not a two-step process involving a structure of type **1c** as had previously been thought. The preference for **1c** over **1b** in the minimal basis set calculations can be explained as an indirect consequence of basis set superposition errors. The small basis set causes C–N contacts that are too short in the bridged structures, and steric interactions with the *ortho* hydrogens artificially favor **1c** over **1b** at these underestimated distances (Figure 2, left).

(26) (a) Kutzelnigg, W. *Isr. J. Chem.* **1980**, *19*, 193. (b) Schindler, M.; Kutzelnigg, W. *J. Chem. Phys.* **1982**, *76*, 1919. (c) Kutzelnigg, W.; Fleischer, U.; Schindler, M. *NMR Basis Principles and Progress*; Springer: Berlin Heidelberg, 1990. (d) Kutzelnigg, W.; Fleischer, U.; Schindler, M. The IGLO-Method: Ab initio Calculations and Interpretations of NMR Chemical Shifts and Magnetic Susceptibilities. In Deuterium and Shift Calculations; Diehl, P., Fluck, E., Günther, H., Kosfeld, R., Seelig, J., Eds.; Springer Verlag: Berlin, 1991; p 165.

(27) Dill, J. D.; Schleyer, P. v. R.; Pople, J. A. *J. Am. Chem. Soc.* **1977**, *99*, 1.

(28) Alcock, N. W.; Greenhough, T. V.; Hirst, D. M.; Kemp, T. J.; Payne, D. R. *J. Chem. Soc., Perkin Trans. 2* **1980**, *1*, 8.

(29) Escudero, F.; Mo, O.; de Paz, J. L. G.; Yáñez, M. *J. Mol. Str. THEOCHEM* **1985**, *120*, 377.

(30) Vincent, M. A.; Radom, L. *J. Am. Chem. Soc.* **1978**, *100*, 3306.

(31) (a) Rømming, C. *Acta Chem. Scand.* **1963**, *17*, 1444. (b) Andresen, O.; Rømming, C. *Acta Chem. Scand.* **1962**, *16*, 1882. (c) Cygler, M.; Przybylska, M.; Elofson, R. *Can. J. Chem.* **1982**, *60*, 2852.

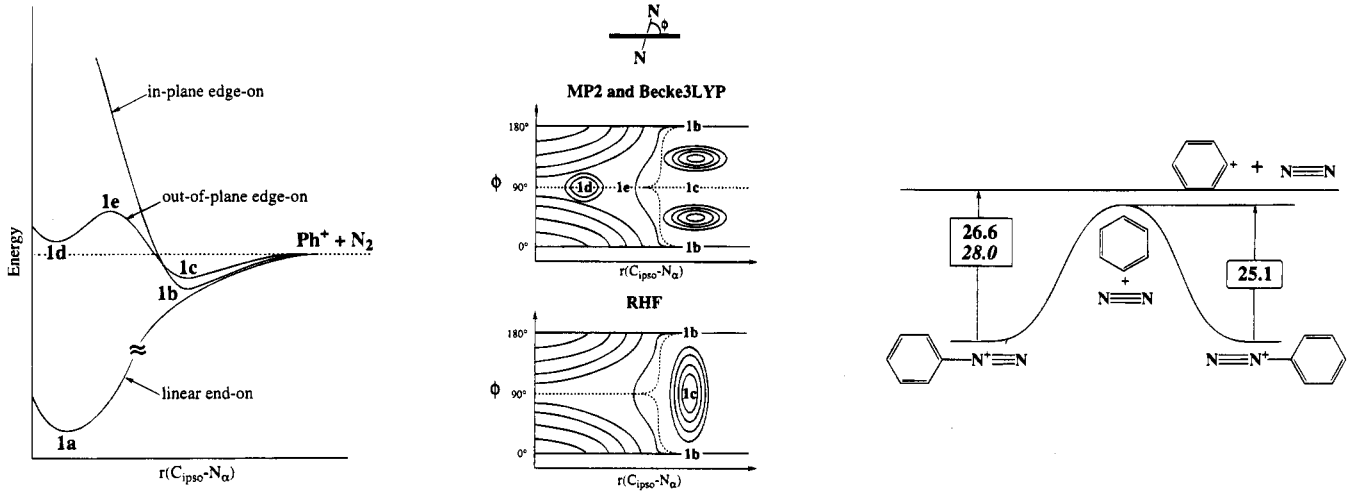


**Figure 2.** Schematic representation of the potential energy profiles for the linear end-on and the two edge-on approaches of $N_2$ to phenyl cation is shown to the left. The schemes shown in the center illustrate the $\phi$ angle dependence of the edge-on approaches. To the right, schematic representations are shown of the potential energy surface for the automerization of **1**; values are those determined at the QCISD(T,fc)/6-31G*//MP2(full)/6-31G* level, and the experimental value is given in italics.

A structure of type **1c** also exists on the MP2 and DFT potential energy surfaces, but *at these correlated levels the character of* ***1c*** *is changed* compared to that at the RHF level. At the RHF/6-31G* level, the imaginary frequencies of 89i and 31i $cm^{-1}$ correspond to normal modes that would lead to automerization and rotation of the $N_2$ group into the molecular plane, respectively. At the MP2 level, however, **1c** is a transition state structure. The imaginary mode (111i $cm^{-1}$) corresponds to the automerization motion just like at the RHF level. The rotation of the $N_2$ group into the molecular plane is now associated with the lowest real vibration (13 $cm^{-1}$). The same scenario occurs at the DFT level where the lowest two frequencies are 121i and 8 $cm^{-1}$. Thus, formally there are two automerization pathways for the $N_\alpha/N_\beta$ exchange in **1a** via the transition state structures **1b** or **1c** as shown schematically in Figure 2 (center). Since these two bridged structures are easily interconverted and nearly isoenergetic, the important result again is that the automerization requires complete disconnection and there is agreement at all levels.

A more severe electron correlation effect on the out-of-plane edge-on approach concerns the existence of another local minimum, **1d**, at the MP2 and DFT levels. The spiro compound **1d** is topologically identical with **1c** but shows much shorter C–N distances. With the emergence of the local minimum **1d**, there also occurs an additional $C_{2v}$ structure, **1e** (Figure 1), which is a transition state structure (MP2 271i; DFT 247i $cm^{-1}$) for disconnection of the $N_2$ group from **1d**. Structure **1d** is found to be almost isoenergetic with the dissociated phenyl cation and $N_2$.

For CN distances beyond that of **1e**, the energy of the out-of-plane edge-on path is lowered and the $C_{2v}$ system goes through a region in the vicinity of **1c** that is bound with respect to free $N_2$ and phenyl cation. If the dissociation of **1e** leads to **1c**, then the system will reduce its symmetry from $C_{2v}$ to $C_s$ and relaxation will lead to **1a**. Thus, the energy difference of 1.0 kcal/mol between **1d** and **1e** is an upper limit for the activation barrier to the interconversion of **1d** to **1a**. An additional $C_s$- or $C_1$-symmetric transition state connecting **1a** and **1d** might exist on the PES with an energy lower than **1e**. We have searched for such a transition state, but it apparently does not exist. The interconversion between **1d** and **1a** therefore does involve **1e** as the transition state, and the symmetry reduction necessary along the path from **1d** via **1e** to **1a** has to occur after passing through **1e** and before **1c** is reached. This discussion points out, of course, that **1d** is not accessible by reaction of $N_2$ with phenyl cation.

The binding energies, $E_b$, are reaction energies for the dissociation of **1a** to form singlet phenyl cation and $N_2$ which is the reaction channel with the lowest activation barrier[32] (Figure 2, right). At our highest level, we find a binding energy for **1a** of 26.6 kcal/mol. Vincent and Radom calculated $E_b$ = 44.3 kcal/mol and argued that this value might be too high by 10–15 kcal/mol. The values in Table 1 show significant variations with the theoretical level. Our systematic studies of the theoretical model dependency of the binding energies of $HN_2^+$,[33] $MeN_2^+$,[6b,e] and $EtN_2^+$[6b] show that binding energies computed at least at the third-order Møller Plesset level and including vibrational zero-point energy corrections reproduce experimental gas phase binding energies sufficiently accurate.

Kuokkanen studied the decomposition of arenediazonium ions (with and without crown ether complexation) in dichloroethane and reported an activation energy for the dissociation of **1a** of 25.8 kcal/mol.[34] Zollinger et al. studied the decomposition of **1a** in 2,2,2-trifluoroethanol in the presence or absence of benzene and determined activation energies of 27.7 and 28.3 kcal/mol, respectively.[35] In fact, Szele and Zollinger measured the rates of the dediazoniations of benzenediazonium ion in 19 different solvents and found that the solvent essentially has no influence on the dissociation rate.[35b–d] The very good agreement between the calculated gas phase and

(32) (a) Bergstrom, R. G.; Landells, R. G. M.; Wahl, G. H., Jr.; Zollinger, H. *J. Am. Chem. Soc.* **1976**, *98*, 3301. (b) Swain, C. G.; Sheats, J. E.; Harbison, K. G. *J. Am. Chem. Soc.* **1975**, *97*, 783.

(33) Glaser, R.; Horan, C. J.; Haney, P. E. *J. Phys. Chem.* **1993**, *97*, 1835.

(34) (a) Kuokkanen, T.; Virtanen, P. O. I. *Acta Chim. Scand. B* **1979**, *33*, 725. (b) Kuokkanen, T. *Acta Chim Scand.* **1990**, *44*, 394.

(35) (a) Burri, P.; Wahl, G. H., Jr.; Zollinger, H. *Helv. Chim. Acta* **1974**, *57*, 2099. (b) Szele, I.; Zollinger, H. *Helv. Chim. Acta* **1978**, *61*, 1721. (c) Lorand, J. P. *Tetrahedron Lett.* **1989**, *30*, 7337. (d) See ref 15, p 199.

**Table 2. Topological Characteristics of the Bond and Ring Critical Points of the Electron Densities of Benzenediazonium Ion[a]**

| no. | A | B | $r_A$ | $r_B$ | $F$ | $\rho$ | $\lambda_1$ | $\lambda_2$ | $\lambda_3$ | $\epsilon$ |
|---|---|---|---|---|---|---|---|---|---|---|
| | | | | | PhNN$^+$, **1a**, at RHF/6-31G* | | | | | |
| 1 | C1 | C5 | 0.763 | 0.628 | 0.584 | 0.322 | −0.694 | −0.560 | 0.210 | 0.240 |
| 2 | C5 | C7 | 0.728 | 0.651 | 0.528 | 0.329 | −0.712 | −0.579 | 0.247 | 0.230 |
| 3 | C7 | C8 | 0.690 | 0.702 | 0.496 | 0.325 | −0.700 | −0.589 | 0.275 | 0.188 |
| 4 | C5 | H10 | 0.706 | 0.369 | 0.657 | 0.291 | −0.813 | −0.806 | 0.477 | 0.008 |
| 5 | C7 | H12 | 0.704 | 0.371 | 0.654 | 0.291 | −0.816 | −0.804 | 0.478 | 0.015 |
| 6 | C8 | H13 | 0.707 | 0.370 | 0.656 | 0.293 | −0.824 | −0.822 | 0.484 | 0.002 |
| 7 | C1 | N2 | 0.434 | 0.986 | 0.306 | 0.216 | −0.290 | −0.230 | 1.245 | 0.258 |
| 8 | N2 | N3 | 0.604 | 0.472 | 0.561 | 0.680 | −1.560 | −1.505 | 0.434 | 0.036 |
| 9[b] | C1 | C8 | 1.317 | 1.382 | 0.480 | 0.020 | −0.014 | 0.086 | 0.096 | |
| | | | | | PhNN$^+$, **1a**, at MP2(full)/6-31G* | | | | | |
| 1 | C1 | C5 | 0.754 | 0.647 | 0.538 | 0.303 | −0.624 | −0.508 | 0.294 | 0.226 |
| 2 | C5 | C7 | 0.714 | 0.676 | 0.514 | 0.312 | −0.646 | −0.535 | 0.318 | 0.207 |
| 3 | C7 | C8 | 0.704 | 0.696 | 0.503 | 0.310 | −0.639 | −0.543 | 0.328 | 0.176 |
| 4 | C5 | H10 | 0.720 | 0.366 | 0.663 | 0.276 | −0.767 | −0.757 | 0.503 | 0.013 |
| 5 | C7 | H12 | 0.720 | 0.366 | 0.663 | 0.279 | −0.778 | −0.771 | 0.508 | 0.008 |
| 6 | C8 | H13 | 0.720 | 0.366 | 0.663 | 0.279 | −0.779 | −0.772 | 0.510 | 0.007 |
| 7 | C1 | N2 | 0.439 | 0.948 | 0.316 | 0.245 | −0.359 | −0.320 | 1.053 | 0.124 |
| 8 | N2 | N3 | 0.613 | 0.523 | 0.539 | 0.577 | −1.239 | −1.236 | 0.866 | 0.003 |
| 9[b] | C1 | C8 | 1.328 | 1.389 | 0.489 | 0.021 | −0.015 | 0.082 | 0.094 | |
| | | | | | $N_2$ at RHF/6-31G* | | | | | |
| 1 | N1 | N2 | 0.539 | 0.539 | 0.500 | 0.711 | −1.699 | −1.699 | 0.638 | 0.000 |
| | | | | | $N_2$ at MP2(full)/6-31G* | | | | | |
| 1 | N1 | N2 | 0.564 | 0.564 | 0.500 | 0.620 | −1.438 | −1.438 | 0.987 | 0.000 |

[a] The $r_A$ and $r_B$ values are the distances in angstroms between the critical point and the atoms A and B, respectively. $F$ is defined as the ratio $r_A/(r_A + r_B)$. The value of the electron density at the critical point, $\rho$, is given in e au$^{-3}$. The curvatures of the electron density at the location of the critical points, $\lambda_i$, are given in e au$^{-5}$. The ellipticity, $\epsilon$, is defined as $\epsilon = \lambda_1/\lambda_2 - 1$. [b] These points are (3,+1) *ring* critical points. All other critical points are (3,−1) *bond* critical points. Ring critical points are characterized by their location with respect to C1, the carbon that carries the diazonio function, and the *para* carbon.

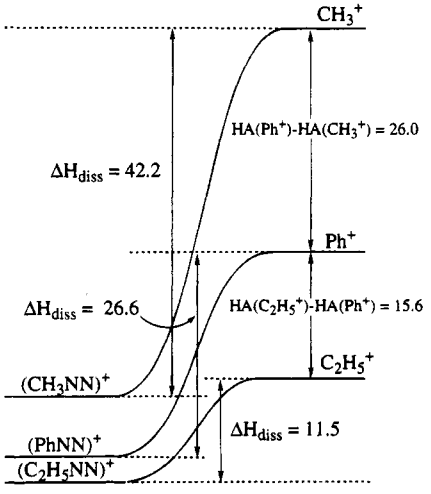


**Figure 3.** Schematic potential energy profiles for the dissociations of benzenediazonium ion (QCISD(T,fc)/6-31G*//MP2-(full)/6-31G*) and of methane- and ethanediazonium ions (MP4(SDTQ)/6-311G(df,p)//MP3(fu)/6-311G(df,p) with reference to the experimental hydride affinities of the free cations.

the measured solution data suggests that it is primarily the intrinsic properties of the benzenediazonium ion that are reflected in the solution chemistry.

The thermodynamic stabilities toward dediazoniation of **1a** and of the prototypical aliphatic systems methane- and ethanediazonium ions[6b,e] are compared in Figure 3 with reference to the hydride affinities of methyl, ethyl, and phenyl cations.[36] Remarkably, the binding energy of methanediazonium ion is 15.6 kcal/mol *larger* than that of **1**. Since aromatic diazonium ions in general are quite stable compared to the highly reactive saturated aliphatic diazonium ions, their clearly distinct reactivities must thus reflect kinetic rather than thermodynamic control.

**Electron Density Distribution in Benzenediazonium Ion and Bonding Model.** Electron density analyses were carried out at the levels RHF/6-31G* and MP2(full)/6-31G* for **1a**. The topological properties of bond and ring critical points are collected in Table 2, and in Table 3 some characteristic values of the electron densities at the nuclei are given. Integrated atomic properties are collected in Table 4. We will discuss the higher level data unless otherwise noted.

The bond critical points of the zero-flux surfaces that partition the C−N and the N−N bonding regions are shifted away from $N_\alpha$. The $F_{CN}$ value, defined as $F_{CN} = r_A/(r_A + r_B)$, is 0.316 for **1a**, that is, the C basin only covers about 30% of the C−N bonding region and the displacements of the N−N bond critical point toward the terminal $N_\beta$ is reflected in the $F_{NN} > 0.5$ value. In free $N_2$, the electron density at the bond critical point is 0.620 e au$^{-3}$ and the curvatures $\lambda_1 = \lambda_2 = -1.438$ e au$^{-5}$. In **1a**, the $\rho$-values are decreased to 0.577 and the curvatures $\lambda_1 = -1.239$ and $\lambda_2 = -1.236$ are less negative compared to free $N_2$. The $F$, $\rho$, and $\lambda$ data show (a) internal $N_2$ polarization that increases the $N_\alpha$ population and (b) radial expansion of the density in the NN bonding region. The integrated phenyl charge of **1a** is +1.003 (Figure 4). While the $N_2$ group is overall nearly neutral, it is internally polarized with $N_\alpha$ being the negative pole.[37]

With the analysis of **1a**, we can draw the important conclusion that the C−N bonding situation in the aromatic diazonium ion is very much the same as in all of

(36) (a) Hydride affinities are 312.1 ($CH_3^+$), 270.5 ($C_2H_5^+$), and 286.1 ($Ph^+$) kcal/mol. Values for methyl and cations are from Berman et al. (Berman, D. W.; Anicich, V.; Beauchamp, J. L. *J. Am. Chem. Soc.* **1979**, *101*, 1239) and are based on the heats of formations listed below. The hydride affinity of phenyl cation differs from the value given by Berman et al. as we considered a more recent value for $\Delta H^f(Ph^+)$. (b) Heats of formation: $\Delta H^f(CH_3^+) = 261.2$ and $\Delta H^f(C_2H_5^+) = 217.1$ Houle, F. A.; Beauchamp, J. L. *Chem. Phys. Lett.* **1977**, *48*, 457. $\Delta H^f(Ph^+) = 272.7 \pm 2.4$ Malinovich, Y.; Lifshitz, C. *J. Phys. Chem.* **1986**, *90*, 2200.

**Table 3. Topological Characteristics of the Electron Densities at the Nuclei of 1a[a,b]**

| | RHF/6-31G* | | | | MP2(full)/6-31G* | | | |
|---|---|---|---|---|---|---|---|---|
| atom | $\rho$ | $\lambda_1$ | $\lambda_2$ | $\lambda_3$ | $\rho$ | $\lambda_1$ | $\lambda_2$ | $\lambda_3$ |
| $N_\alpha$ | 191.733 | −322.546 | −322.545 | −322.543 | 191.607 | −322.294 | −322.293 | −322.292 |
| $N_\beta$ | 192.573 | −324.023 | −324.021 | −324.012 | 192.523 | −323.921 | −323.920 | −323.915 |
| $C_{ipso}$ | 118.063 | −145.423 | −145.420 | −145.420 | 118.057 | −145.412 | −145.410 | −145.410 |
| $C_{ortho}$ | 118.155 | −145.547 | −145.545 | −145.545 | 118.097 | −145.471 | −145.471 | −145.470 |
| $C_{meta}$ | 118.141 | −145.533 | −145.532 | −145.532 | 118.120 | −145.503 | −145.501 | −145.501 |
| $C_{para}$ | 118.192 | −145.595 | −145.592 | −145.592 | 118.131 | −145.517 | −145.515 | −145.515 |
| $H_{ortho}$ | 0.414 | −6.337 | −6.331 | −5.887 | 0.405 | −6.106 | −6.101 | −5.481 |
| $H_{meta}$ | 0.416 | −6.378 | −6.370 | −5.926 | 0.409 | −6.169 | −6.163 | −5.535 |
| $H_{para}$ | 0.418 | −6.411 | −6.404 | −5.954 | 0.410 | −6.189 | −6.183 | −5.555 |

[a] See legend to preceding table. [b] Electron densities $\rho$ and curvatures $\lambda$ given for N and C are given in units of $10^3$ e/au$^{-3}$ and $10^3$ e/au$^{-5}$, respectively.

**Table 4. Integrated Atomic Charges, First Atomic Moments, and Atom Stabilities of 1a**

| | RHF/6-31G* | | | | MP2(fu)/6-31G* | | |
|---|---|---|---|---|---|---|---|
| atom | charge | $\pi$-pop. | $\mu$ | KE | charge | $\mu$ | KE |
| $C_{ipso}$ | +0.138 | 1.190 | 0.740 | 37.75819 | +0.269 | 0.676 | 37.87060 |
| $C_{ortho}$ | +0.076 | 0.896 | 0.357 | 37.83443 | +0.011 | 0.316 | 38.03449 |
| $C_{meta}$ | +0.063 | 0.937 | 0.217 | 37.82893 | +0.005 | 0.221 | 38.04457 |
| $C_{para}$ | +0.018 | 0.844 | 0.121 | 37.86649 | −0.004 | 0.192 | 38.04483 |
| $H_{ortho}$ | +0.114 | 0.018 | 0.126 | 0.57008 | +0.147 | 0.143 | 0.54837 |
| $H_{meta}$ | +0.103 | 0.019 | 0.126 | 0.57627 | +0.141 | 0.143 | 0.55404 |
| $H_{para}$ | +0.106 | 0.017 | 0.126 | 0.57705 | +0.134 | 0.143 | 0.55682 |
| $N_\alpha$ | −0.540 | 1.293 | 0.345 | 54.99035 | −0.374 | 0.478 | 55.02630 |
| $N_\beta$ | +0.558 | 0.918 | 0.883 | 53.93115 | +0.363 | 0.733 | 54.27574 |
| Σ | +0.992 | 8.006 | | 338.74265[a] | +0.992 | | 340.13723[a] |
| Σ(H) | +0.540 | | | 2.86975 | +0.710 | | 2.76164 |
| Σ(C) | +0.434 | | | 226.95140 | +0.297 | | 228.07355 |
| *o*-CH | +0.190 | 0.914 | | 38.40451 | +0.158 | | 38.58286 |
| *m*-CH | +0.166 | 0.956 | | 38.40520 | +0.146 | | 38.59861 |
| *p*-CH | +0.124 | 0.861 | | 38.44354 | +0.130 | | 38.60165 |
| Ph | +0.974 | 5.795 | | 229.82115 | +1.003 | | 230.83519 |
| $N_2$ | +0.018 | 2.211 | | 108.92150 | −0.011 | | 109.30204 |

[a] Dipole moments ($\mu$) and kinetic energies (KE) are in atomic units. [b] Deviations between the molecular energy calculated directly and determined *via* the sum of the negative atom kinetic energies: $PhNN^+$, **1a**, RHF = 0.27 kcal/mol; MP2 = 183.19 kcal/mol.

the aliphatic diazonium ions studied previously.[6] In general, electron density analysis (EDA) of all types of


diazonium ions reveals that most of the positive charge resides on the hydrocarbon fragment, and not on the $N_2$ group. Diazonium ions can best be thought of as carbenium ions closely associated with an $N_2$ group that is internally polarized in the fashion $N_\alpha^{\delta-}-N_\beta^{\delta+}$. The usual Lewis–Kekulé notations are inadequate since they imply electron density transfer from $N_2$ to the hydrocarbon fragment and electron depletion at $N_\alpha$. Our bonding model implies dative N→C bonding, and it is fully consistent with the properties of the electron density distributions in diazonium ions irrespective of charge and nature of the R group.[6] C–N bonding is attributed to the combined stabilization resulting from density accumulation in the CN bonding region and the electrostatic attraction between the internally polarized $N_2$ group and the positive charge on the hydrocarbon fragment.[6b,7b]

(37) The absolute charges assigned to $N_\alpha$ (−0.540 (RHF), −0.374 (MP2)) and $N_\beta$ (+0.558 (RHF), +0.363 (MP2)) differ at the RHF and MP2 levels as do the associated N atom dipole moments. We discussed these effects of electron correlation previously in detail. In bonding regions characterized by small gradients along the bonding axis, small changes in the electron density distribution may result in large changes of atom populations *and* atom dipoles and *both* of these quantities need to be considered together to correctly appreciate electron correlation effects (see ref 7c).

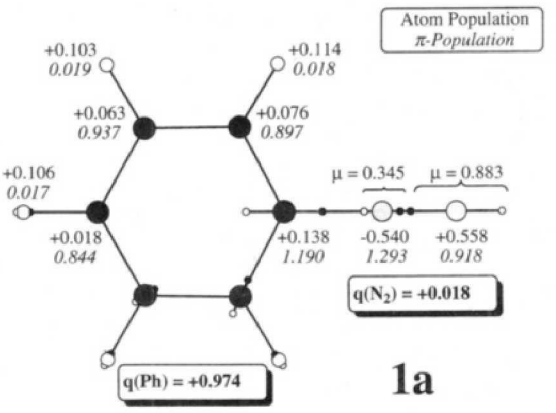


**Figure 4.** Integrated atom and fragment charges, $\pi$ populations, and atomic dipole moments (au) as determined with the RHF/6-31G* electron densities of **1**. The vectors of the atom dipole moments $\mu$ are superimposed on the molecules and they are directed from unfilled (○) to the filled (●) markers.

It is important to note that the EDA representation reflects the *total* electron density which is observable and can in principle be measured experimentally. While the $\sigma$- and $\pi$-components of the electron density are not "observable" in the strictest sense, the concept of $\sigma/\pi$ separation has been and remains successful and it is central to all models invoking dative and back-dative bonding. We determined the integrated $\pi$ populations (Table 4) as we have done before for other diazonium ions.[6a,c] The $\pi$ population of the $N_2$ group (2.21) shows that $\sigma$-dative C←N bonding is accompanied by C→N $\pi$-back-dative bonding of nearly equal magnitude.

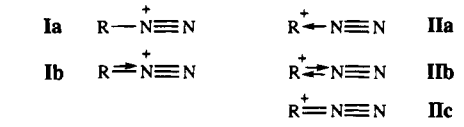


The $\sigma$-dative term is much smaller than unity, thereby clearly favoring representation **IIa** over **Ia**. The notations **Ib** and **IIb** are representations that also indicate $\pi$-back-dative bonding. The theoretical analysis shows similar amounts of $\sigma$-donation and $\pi$-back-donation resulting in CN bonding with little overall charge transfer as is best reflected by notation **IIb** which is equivalent with the hypervalent[38] notation **IIc** (since electrons are indistinguishable). The R group is not required to be unsaturated for such $\pi$-back-bonding to occur.[6a] Considering the *overall charge transfer* as the only criterion, **IIa**–**IIc** all are equally valid and representations **I** are inadequate.

**Consistency of the Electron Density Model with Substituent and Reaction Constants. (1) Diazonium Function Substituent Constant.** Lewis and Johnson[39] measured the ionization constants of *p*-hydroxy- and *p*-aminobenzenediazonium ions and showed the diazonium function to be the most powerful "electron-withdrawing" and deactivating substituent with $\sigma_p^- = 3$. Clearly, the results of our electron density analysis are fully compatible with these physical organic studies in that the substituent "-$N_2^+$" withdraws virtually a full charge to become overall nearly neutral.

**(2) Reaction Constants in Dual Substituent Parameter Relations.** Zollinger[40a] recently provided a mechanistic interpretation of reactions with opposing signs of field (inductive) and resonance constants in the dual substituent parameter (DSP) treatments of Taft, Yukawa-Tsuno, and Godfrey. The Taft equation, $\log(k_x/k_o) = \rho_F\sigma_F + \rho_R\sigma_R$, is the most widely applied DSP relationship, and the following discussion is cast in terms of this equation (other formalisms lead to the same conclusions). Only a very few reactions are known with opposing signs of $\rho_F$ (field reaction constant) and $\rho_R$ (resonance reaction constant). These 14 reactions were summarized and discussed by Zollinger,[40a] and they include the dediazoniations of arenediazonium ions in water, in 1,2-dichloroethane[40b] (in the absence or presence of crown ethers), and in TFE.[40c] For all of these dediazoniations it is known that $\rho_F$ is negative ($<-3.5$), that $\rho_R$ is positive ($>2.2$), and that $|\rho_F| > |\rho_R|$.

For the linear unimolecular association (dissociation), the $a_1$–$a_1$ interaction between the $N_2$ $\sigma$ lone pair and the phenyl cation $sp^2$ LUMO is increased by inductively withdrawing substituents ($\sigma_F > 0$) and should give rise to a substantial positive (negative) $\rho_F$ value for the association (dissociation). On the basis of orbital interaction analysis, Zollinger argued that *a $\rho_R$ constant of opposing sign is plausible* since $\pi$-electron donating substituents should slow (fasten) the association (dissociation) reaction and that these $\pi$-interactions should be less than the $\sigma$-interactions ($|\rho_F| > |\rho_R|$). Zollinger points out that his conclusions cannot be demonstrated experimentally but they are supported and fully consistent with the theoretical result that $\sigma$-dative C←N bonding is accompanied by C→N $\pi$-back-dative bonding. The importance of $\pi$-back-bonding also is consistent with the finding that the $\pi$ populations at the *ortho* and *para* positions are less than at the *meta* positions.

The DSP analysis of the automerization of benzenediazonium ion results in reaction constants ($\rho_F = -3.4$ and $\rho_R = 2.5$) that agree very closely with the respective values for the dediazoniations.[40a] This finding is fully consistent with the conclusion that automerization requires essentially complete $N_2$ disconnection (*vide supra*).

**Table 5. Properties of Noble Gases and Computed Data for the (Ph–E)$^+$ Systems**

| parameter[a] | He | Ne | Ar | Xe |
|---|---|---|---|---|
| ionization potential | 24.587 | 21.564 | 15.759 | 12.130 |
| $r_{vdW}$, viscosity measurement, 0 °C | 1.10 | 1.30 | 1.83 | 2.45 |
| $r_{vdW}$, crystal lattice data | 1.79 | 1.60 | 1.92 | 2.18 |
| polarizability, α | 1.384[b] | 2.669[c] | 11.08[c] | 27.16[c] |
| $d$(C–E) | 2.866 | 2.396 | 2.623 | 2.092[d] |
| IC(E) RHF | −0.001 | −0.004 | +0.012 | |
| $\mu$(E) | −0.009 | +0.085 | +0.094 | |
| IC(E) MP2 | −0.001 | −0.002 | +0.054 | |
| $\mu$(E) | 0.009 | 0.097 | +0.084 | |

[a] Ionization potentials in eV (from ref 41), distances in Å, integrated charges (IC) and atom dipole moments $\mu$ in atomic units. [b] Calculated value from ref 46a. [c] Experimental polarizabilities in atomic units from ref 46b. [d] Experimental value from ref 43.

**Internal $N_2$ Polarization and C–N Bonding: Comparison to Noble Gas Systems (Ph–E)$^+$.** On the basis of integrated atom properties, we previously argued for the importance of contributions of both dative bonding and charge–dipole interactions to C–N bonding. This question can be pursued further by consideration of the ions (Ph–E)$^+$ in which E is a noble gas atom.[41] The ion (Ph–He)$^+$ was experimentally observed in the $\beta$-decay studies of tritiated benzenes by Speranza.[42] Frohn et al.[43] succeeded in the first structural characterization of a molecule with a phenyl–Xe bond, the ion [MeCN–Xe–$C_6F_5$]$^+$, and the existence of the closely related ion [HCN–Ar–F]$^+$ was recently predicted.[44] As can be seen from the data provided in Table 5, only the lighter three of the noble gases have ionization potentials[45] that are *higher* than that of $N_2$ (15.576 eV), and we thus focus on the study of the phenyl cation noble gas complexes (Ph–E)$^+$ where E = He, Ne, or Ar. Pertinent results are summarized in Figure 5.

The phenyl portions of the benzene noble gas cations show structural parameters very similar to those of the phenyl cation. The Ph–E bonds do not change steadily from He to Ne and Ar, reflecting trends of both the polarizability and the van der Waals (vdW) radii of E.

(38) For discussions of hypervalency in diazo compounds, see refs 6e and 7c and literature cited there.

(39) (a) Lewis, E. S.; Johnson, M. D. *J. Am. Chem. Soc.* **1959**, *81*, 2070. (b) Note that the $\sigma$ values derived from ionization constants of other systems or from rate data vary. In any case, all $\sigma$ values determined for the diazonium function are larger than 1.8.

(40) (a) Zollinger, H. *J. Org. Chem.* **1990**, *55*, 3846. (b) Nakazumi, H.; Kitao, T.; Zollinger, H. *J. Org. Chem.* **1987**, *52*, 2825. (c) Ravenscroft, M. D.; Zollinger, H. *Helv. Chim. Acta* **1988**, *71*, 507.

(41) (a) Review: Frenking, G.; Cremer, D. *Struct. Bonding* **1990**, *73*, 17. (b) Frenking, G.; Koch, G.; Reichel, F.; Cremer, D. *J. Am. Chem. Soc.* **1990**, *112*, 4240.

(42) Speranza, M. *Chem. Rev.* **1993**, *93*, 2933.

(43) (a) Frohn, H. J.; Jakobs, S.; Henkel, G. *Angew. Chem., Int. Ed. Engl.* **1989**, *28*, 1506. (b) Frohn, H. J.; Klose, A.; Henkel, G. *Angew. Chem., Int. Ed. Engl.* **1993**, *32*, 99. (c) The Xe–C bond distance is 2.092 Å in the ion [MeCN–Xe–$C_6F_5$]$^+$, and it is well within the sum of the van der Waals radii of 3.880 Å. The electron-withdrawing fluorine substituents, the high polarizability of Xe, and the lower ionization potential of Xe all contribute to the significant shortening of the Ph–Xe bond compared to the other noble gas systems.

(44) Wong, M. W.; Radom, L. *J. Chem. Soc., Chem. Commun.* **1989**, 719.

(45) *CRC Handbook of Chemistry and Physics*, 71st ed.; CRC Press: Boca Raton, FL, pp 10–210 ff.

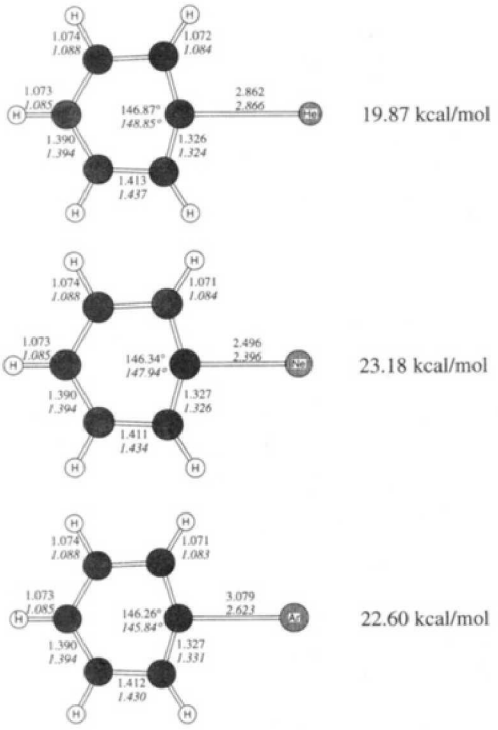


**Figure 5.** RHF/6-31G* and the MP2(full)/6-31G* (in italics) structures of the $Ph^+-E$ (E = He, Ne, Ar) systems. Binding energies as determined at the MP2(full)/6-31G* level.

The polarizability increases from He to Ne and Ar,[46] but the trend in the van der Waals radii[47] is less clear. While vdW radii determined by viscosity measurements indicate a steady increase, the crystal lattice determined data give higher values for He to Ar and indicate a minimal vdW radius for Ne. The vdW radii determined by the latter method seem more appropriate as they are consistent with the calculated trend of the $Ph^+-E$ bond lengths.

The binding energies for the systems with He, Ne, and Ar all fall in the range of 21 ± 2 kcal/mol, and they remain about 30% lower than for benzenediazonium ion. Topological electron density analysis shows (Table 5) that the E atom essentially remains neutral in the complexes $(Ph-E)^+$, just like the $N_2$ group in **1a**. The placement of an overall neutral atom (He, Ne, Ar) or molecule ($N_2$) in the electric field of phenyl cation results in stabilization in all cases. The significantly higher binding energy of the diazonium ion thus can be attributed to the additional stabilization gained by the favorable electrostatic interaction between the charge distribution of the phenyl cation fragment and of the induced dipole within the $N_2$ group. The atomic dipole moments of the noble gas atoms are marginal in comparison to the internal polarization of $N_2$. The $N_2$ fragment also is better suited for dative bonding because of its sp-hybridized lone pair.

**$N_2$ Group Effects on the Electron Density Distribution within the Phenyl Group.** With C–N linkage in benzenediazonium ion being of the same nature as in all other types of diazonium ions, the pertinent issue concerning the electron density distribution in **1** thus relates to the question as to how the positive charge is apportioned throughout the phenyl group. Benzenediazonium ions are susceptible to electrophilic attack at the *meta* position and to nucleophilic attack on the terminal

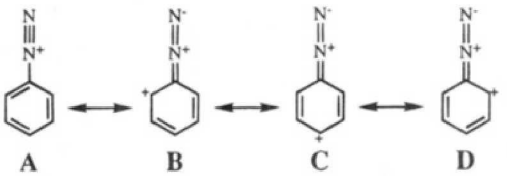


nitrogen,[48] at the ipso-carbon,[49] and at the *ortho* and *para* positions of the aromatic ring.[50] Since "qualitative theories of aromatic substitution have long been based on the idea of Coulombic attractions between the attacking positive reagent and the electron density of different positions of the aromatic ring" [51a] and considering this reaction chemistry and the overall neutrality of the $N_2$ group, one would be inclined to assume that the diazonium substituent causes electron density depletion particularly at the *ortho* and *para* positions as indicated by the *formal* charges of resonance forms **B**–**D**. The electron density analysis demonstrates that this line of reasoning does not hold true.

The charges on the *ortho*, *meta*, and *para* carbons are all extremely small ($|q(C)| < 0.011$), and most of the positive charge resides on the hydrogens (Table 4 and Figure 4). Comparison of the CH group charges *does not* indicate larger depletions of electron density at the *ortho* and *para* positions, but instead the C-atom and CH group (*ortho* 0.158, *meta* 0.146, *para* 0.130) charges decrease with increased distance from the site of the $N_2$ substituent. While the total charges of the CH groups do not parallel the diazonium substituent's directing effects, one might expect these directing effects to be reflected in the $\pi$-system since it is the $\pi$ populations that have been related successfully to the directing effects in HMO theory. We determined the $\pi$ components of the integrated populations (Table 4), and indeed, these $\pi$ populations do indicate decreases in density in the *ortho* and *para* positions and a greater $\pi$-density at the *meta* positions. We determined the $\pi$ components of the integrated populations (Table 4), and indeed, these $\pi$ populations do indicate decreases in density in the *ortho* and *para* positions and a greater $\pi$ density at the *meta* positions. Bader recently suggested[51b] that the correlation of reactivity indices with the $\pi$ populations is related to the domination of the atomic quadrupole moment by the $\pi$ populations.

Nucleophilic substitutions at $C_{ipso}$ and nucleophilic additions to $N_\beta$ are exothermic, and in these cases, it is

(46) (a) Rice, J. E.; Taylor, P. R.; Lee, T. J.; Almlöf, J. *J. Chem. Phys.* **1991**, *94*, 4972. (b) Kumar, A.; Meath, W. J. *Can. J. Chem.* **1985**, *63*, 1616.

(47) Sets of van der Waals radii can and have been determined by various methods, and they differ greatly in relative and absolute values: *Argon, Helium and the Rare Gases*; Cook, G. A., Ed.; Vol. 1; Wiley (Interscience Publishers): New York, 1961; p 13. The van der Waals data selected for the present study were ascertained by separation of the atoms at very low temperatures in crystal lattices.

(48) Examples of nucleophilic attack include the following: (a) Haub, E. K.; Lizano, A. C.; Noble, M E. *J. Am. Chem. Soc.* **1992**, *114*, 2218. (b) Carroll, J. A.; Fisher, D. R.; Canham, G. W. R.; Sutton, D. *Can. J. Chem.* **1974**, *52*, 1914. (c) Einstein, F. W. B.; Sutton, D.; Vogel, P. L. *Can. J. Chem.* **1978**, *56*, 891. (d) See also ref 13.

(49) (a) Replacement by $F^-$, for a review, see: Suschitzky, H. *Adv. Fluorine Chem.* **1965**, *4*, 1. (b) Replacement by $OH^-$: Dreher, E.-L.; Niederer, P.; Rieker, A.; Schwarz, W.; Zollinger, H. *Helv. Chim. Acta* **1981**, *64*, 488.

(50) (a) Lewis, E. S.; Johnson, M. D. *J. Am. Chem. Soc.* **1960**, *82*, 5399. (b) Lewis, E. S.; Johnson, M. D. *J. Am. Chem. Soc.* **1960**, *82*, 5408. (c) Lewis, E. S.; Chalmers, D. J. *J. Am. Chem. Soc.* **1971**, *93*, 3267.

(51) Citation and leading references can be found in the following: (a) Aromatic Substitution. Chapter 11 in Streitwieser, A., Jr. *Molecular Orbital Theory for Organic Chemists*; Wiley & Sons: New York, 1961. (b) Bader, R. F. W.; Chang, C. *J. Phys. Chem.* **1989**, *93*, 2946, 5095.

Table 6. $^{13}C$ and $^{15}N$ NMR Chemical Shifts and Principal Shielding Values of Benzenediazonium Ion[a]

| | IGLO (DZ) | IGLO (Basis II) | | | | | | | expt[b] |
|---|---|---|---|---|---|---|---|---|---|
| atom | $\delta$ | $\sigma_{11}$ | $\sigma_{22}$ | $\sigma_{33}$ | $\sigma^d$ | $\sigma^p$ | $\sigma$ | $\delta$ | $\delta$ |
| | | | | **1a** | | | | | |
| $C_{ipso}$ | 114.17 | 127.37 | 112.29 | 1.65 | 264.04 | −183.61 | 80.44 | 112.18 | 115.8 |
| $C_{ortho}$ | 137.19 | 190.15 | 35.77 | −52.30 | 255.26 | −197.39 | 57.88 | 134.74 | 134.5 |
| $C_{meta}$ | 130.78 | 197.69 | 35.58 | −52.04 | 262.85 | −202.44 | 60.41 | 132.21 | 134.2 |
| $C_{para}$ | 150.17 | 196.05 | 13.77 | −86.61 | 256.65 | −215.58 | 41.07 | 151.55 | 144.5 |
| $N_\alpha$ | −198.41 | 402.82 | −162.02 | −162.32 | 321.32 | −295.16 | 26.16 | −152.95 | −150.2 |
| $N_\beta$ | −53.66 | 203.65 | −211.68 | −280.82 | 314.72 | −411.00 | −96.29 | −30.50 | −57.2 |
| | | | | Phenyl Cation | | | | | |
| $C_{ipso}$ | 323.2 | −228.75 | −24.28 | −193.33 | 259.70 | −408.48 | −148.78 | 341.4 | |
| $C_{ortho}$ | 104.3 | 153.15 | 59.31 | 78.14 | 260.80 | −163.93 | 96.86 | 95.8 | |
| $C_{meta}$ | 149.8 | 157.53 | −6.40 | −18.26 | 256.82 | −212.53 | 44.29 | 148.3 | |
| $C_{para}$ | 134.3 | 196.37 | −62.57 | 43.61 | 269.38 | −202.24 | 59.13 | 133.5 | |

[a] Experimental and theoretical $^{13}C$ chemical shifts in ppm with respect to TMS. Experimental $^{15}N$ chemical shifts in ppm upfield from $H^{15}NO_3$, and theoretical shifts calculated with reference to $NH_3$ and converted to the $H^{15}NO_3$ standard ($\delta(NH_3) = -375.8$ with respect to $H^{15}NO_3$). [b] See ref 59.

in agreement with Hammond's postulate to relate the reactivity to the charge distribution in the diazonium ion. In contrast, the formation of the Meisenheimer complex is greatly endothermic and the regiochemistry must reflect the directing effects of the diazonium substituent *in the Meisenheimer complex* and to a much lesser extent those in the free diazonium ion. The finding that the benzene ring $\pi$ populations parallel the regioselectivity is thus nothing more than a useful empirical rule but it *does lack* a solid theoretical foundation and has no implications whatsoever as to the charge distribution in the free diazonium ion.

Two prominent structural features of **1a** concern the NN bond length and the $C_{ipso}$ ring angle.[52] It has long been known that the NN bond lengths in diazonium ions are *shorter* than those in free $N_2$.[53] This feature clearly is totally inconsistent with severe electron depletion of the $N_2$ group, but it is explained by the electron density based bonding model as the result of the increased internal N−N bond polarization. The angles in the phenyl ring are sensitive to the nature of attached substituents: Substituents that deplete $C_{ipso}$ of electron density exert a small angle-widening effect to increase this C atom's s-character.[54] In the extreme case of phenyl cation,[55] the ring angle at $C_{ipso}$ is widened to 146.9° and the respective values in **1b** and **1c** are very similar. The ion **1a** shows a smaller but substantial widening (125.1°) of the angle at the positively charged (0.138) $C_{ipso}$ atom.

**Electron Density Distribution and $^{13}C$ and $^{15}N$ NMR Chemical Shifts.** The electron density based bonding model was tested via examination of its consistency with the NMR spectroscopic properties of diazonium ions. Theoretically derived NMR chemical shifts and shielding parameters are summarized in Table 6 together with measured data.

**(1) Theoretical versus Experimental $^{13}C$ and $^{15}N$ Chemical Shifts.** The Basis II data result in excellent agreement with the experimental $^{13}C$ chemical shifts of the phenyl ring carbons. The *ipso* carbon has an extreme upfield shift relative to benzene ($\delta$ = 128.5 ppm), the carbon in the *para* position relative to the $N_2$ substituent shows a marked downfield shift to around $\delta$ = 150 ppm, and the *ortho* and *meta* carbons exhibit almost equivalent chemical shifts with $\delta = 134 \pm 2$ ppm. At Basis II, the calculated N chemical shift for $N_\alpha$ is −152.95 ppm (upfield from $H^{15}NO_3$) and the shift for $N_\beta$ is −30.50 ppm. $N_\alpha$ and $N_\beta$ were unequivocally assigned using labeled compounds to the signals at $\delta = -143 \pm 3$ and $\delta = -55 \pm 5$ ppm, respectively, relative to external 1 M $H^{15}NO_3$ in $D_2O$.[56] The relative position of these signals agrees well with experiment while the absolute values deviate somewhat.[57] The fact that theory is so well capable of reproducing the NMR chemical shifts excludes computational deficiencies in the determination of the electron density distributions. The following analysis of the $^{13}C$ and $^{15}N$ NMR demonstrates that there is no relation, and thus also no conflict, between the measured NMR chemical shifts and the theoretically determined electron density distribution.

**(2) Diamagnetic and Paramagnetic Shielding.** The diamagnetic shielding, $\sigma^d$,[58] depends on the electron

(52) For a detailed discussion of such distortions, see: Horan, C. J.; Barnes, C. L.; Glaser, R. *Chem. Ber.* **1993**, *126*, 243.

(53) This feature is common to aromatic and aliphatic diazonium ion. Compare the discussion in ref 9b.

(54) (a) Bock, H.; Ruppert, K.; Näther, C.; Havlas, Z.; Herrmann, H.-F.; Arad, C.; Göbel, I.; John, A.; Meuret, J.; Nick, S.; Rauschenbach, A.; Seitz, W.; Vaupel, T.; Solouki, B. *Angew. Chem., Int. Engl.* **1992**, *31*, 550. (b) Domenicano, A.; Vaciago, A.; Coulson, C. A. *Acta Crystallogr.* **1975**, *B31*, 221. (c) Domenicano, A.; Vaciago, A.; Coulson, C. A. *Acta Crystallogr.* **1975**, *B31*, 1630. (d) Domenicano, A.; Vaciago, A. *Acta Crystallogr.* **1979**, *B35*, 1382. (e) Domenicano, A.; Murray-Rust, P.; Vaciago, A. A. *Acta Crystallogr.* **1983**, *B39*, 457. (f) Domenicano, A. *Structural Substituent Effects in Benzene Derivatives.* In *Accurate Molecular Structures—Their Determination and Importance*; Domenicano, A.; Hargittai, I.; IUCr/Oxford University Press: Oxford, 1992.

(55) For prior ab initio calculations of phenyl cation, see: (a) Dill, J. D.; Schleyer, P. v. R.; Binkley, J. S.; Seeger, R.; Pople J. A.; Haselbach, E. *J. Am. Chem. Soc.* **1976**, *98*, 5428. (b) Dill, J. D.; Schleyer, P. v. R.; Pople, J. A. *J. Am. Chem. Soc.* **1977**, *99*, 1. (c) Schleyer, P. v. R.; Kos, A. J.; Raghavachari, K. *J. Chem. Soc., Chem Commun.* **1983**, 1296. (d) Krogh-Jespersen, K.; Chandrasekhar, J.; Schleyer, P. v. R. *J. Org. Chem.* **1980**, *45*, 1608. (e) Apeloig, Y.; Arad, D. *J. Am. Chem. Soc.* **1985**, *107*, 5285. (f) Uggerud, E.; Arad, D.; Apeloig, Y.; Schwarz, H. *J. Chem. Soc., Chem Commun.* **1989**, 1015. (g) Tasaka, M.; Ogata, M.; Ichikawa, H. *J. Am. Chem. Soc.* **1981**, *103*, 1885. (h) Reference 10d.

(56) (a) Duthaler, R. O.; Forster, H. G.; Roberts, J. D. *J. Am. Chem. Soc.* **1978**, *100*, 4974. (b) Casewit, C.; Roberts, J. D.; Bartsch, R. A. *J. Org. Chem.* **1982**, *47*, 2875. (c) The ranges given for the chemical shifts reflect dependencies on counterion and solvent. (d) As for H and C chemical shifts, the signs of the $\delta$(N) values are chosen such that $\delta$ increases with decreasing shielding.

(57) It is well-known that the IGLO method exaggerates the paramagnetic effects of nitrogens involved in double and triple bonds. Differences between experiment and theory of up to 100 ppm arise in cases where two nitrogen atoms are next neighbors. See refs 26c, 26d, and (a) Schindler, M. *Magn. Reson. Chem.* **1988**, *26*, 394. (b) Schindler, M. *J. Am. Chem. Soc.* **1988**, *110*, 6623. (c) Schindler, M. *J. Am. Chem. Soc.* **1987**, *109*, 5950. (d) Sieber, S.; Schleyer, P. v. R. *J. Am. Chem. Soc.* **1993**, *115*, 6987.

(58) For further discussion, see: (a) Lambert, J. B.; Shurvell, H. F.; Lightner, D. A.; Cooks, R. G. *Introduction to Organic Spectroscopy*; Macmillan Publishing Company: New York, 1987. (b) Wehrli, F. W.; Marchand, A. P.; Wehrli, S. *Interpretation of Carbon—13 NMR Spectra*; John Wiley & Sons: New York, 1989.

density around the nucleus. For hydrogens, $\sigma^d$ dominates the shielding and electron-deficient hydrogens *do show* a marked downfield shift. For nuclei with nonspherical electron distributions, such as C and N, the paramagnetic shielding, $\sigma^p$, becomes important. The shielding components $\sigma^p$ and $\sigma^d$ have opposite signs. The shielding $\sigma^p$ is a complicated function

$$\sigma^p \propto (\langle 1/r^3 \rangle Q_{ij})/\Delta E$$

that mainly depends on (a) the average excitation energy $\Delta E$, (b) a term $<r^{-3}>$ weighing the contributions from electrons in a volume element at distance $r$ from the nucleus, and (c) a parameter $Q_{ij}$ that has been related to bond order.[58a]

Frequently, NMR data are interpreted with the implied or explicitly stated assumption that there exists a relation between the charges and the chemical shifts. Many such attempts have been documented for diazonium ions on the basis of $^{13}C$ NMR[59,60] and $^{15}N$ NMR[56b] spectroscopy. The basic question is whether such interpretations are valid or not, and we address this question for benzenediazonium ion.

**(3) Analysis of the Computed $^{13}C$ NMR Parameters.** For all of the phenyl ring carbons, $\sigma^d(C)$ consistently assumes values that fall in a narrow interval around $259 \pm 5$. The paramagnetic component, however, varies greatly from $-183.6$ to $-215.6$, and it is thus $\sigma^p(C)$ that has the major influence on the C chemical shift. Thus, the measured $^{13}C$ NMR chemical shifts do not reflect the diamagnetic shielding differences, which are thought to be related to charges, and the $^{13}C$ NMR chemical shifts are therefore not inconsistent with the density-based bonding model.

While $\delta(^{13}C)$ is certainly not correlated with atomic charges, the question remains as to whether the computed diamagnetic contributions are related to the charges of the carbon atoms or the CH groups. However, no such relation exists. The positive C charges decrease with distance from $C_{ipso}$, and since the same is true for the H charges, the CH charge pattern must fall in suit. Yet, the $\sigma^d$ values are similar for the *ortho* (255.26) and *para* (256.65) carbons while the *meta* carbon has a higher $\sigma^d$ shielding (265.85). The fact that there is no correlation between $\sigma^d$ and the integrated charges (or the charges from other population methods) is easily explained. It is obvious that equal amounts of electrons in small volume elements at different locations with respect to the nucleus contribute differently to the shielding. Electrons in the bonding regions, for example, are far removed from the nuclei and contribute less than do electrons near the nuclei. In the determination of the atom charges with the topological method or with any other method, this distribution information is lost and therefore the charges derived from population analysis cannot reflect shielding. In the other extreme, one might be tempted to correlate the electron density at the nucleus with the $\sigma^d$ term following the philosophy that the core density reflects atomic charge.[61] We determined the electron densities at the positions of the nuclei together with their three principal curvatures, and the results are summarized in Table 3. For the C atoms, the $\rho$ values at the nuclei, the contact densities, deviate less than 1 per mill and they clearly do not correlate with the $\sigma^d$ data. These few examples suffice to show that $\sigma^d$ is not a simple function of the population-derived atom charge nor of the density at the nucleus, and thus it also is not and cannot be a function of "atomic charge" alone. The diamagnetic shielding depends on the electron density *distribution* around the atom; the computed $\sigma^d$ values reflect this *distribution* information and they are therefore of an entirely different nature than are populations or contact densities.

**(4) Analysis of the Computed $^{15}N$ NMR Parameters.** As with the $^{13}C$ shieldings, we find that $\sigma^d(N)$ varies relatively little (321.3 for $N_\alpha$, 314.7 for $N_\beta$) and that the large difference in the $N_\alpha$ and $N_\beta$ chemical shifts are the result of large differences in their *paramagnetic* shieldings ($-295.2$ for $N_\alpha$, $-411.0$ for $N_\beta$). For the N atoms, the larger (less negative) chemical shift is observed for the atom that is assigned the higher electron population. Moreover, $\sigma^d(N_\alpha)$ and $\sigma^d(N_\beta)$ indicate a larger diamagnetic shielding for $N_\alpha$ than for $N_\beta$. For the same reasons as discussed for the $^{13}C$ NMR data, these results *cannot* be taken as evidence for the internal polarization of the $N_2$ group and thus neither supports the density-based bonding model nor is it in conflict with it.

## Conclusion

The concept of "dative bonding" has been central to discussions of complex chemistry throughout this century. Inorganic textbooks discuss dative bonding between Lewis bases (D, donor) and Lewis acids (A, acceptor) in the introduction to complex chemistry and dative bonds are indicated by the "D→A" bond symbol. Cotton and Wilkinson, for example, state that "it is possible to regard even covalent compounds - such as methane - from the donor-acceptor point of view" but continue to recognize that "it is not a particularly profitable or realistic way of looking at such molecules".[62] By and large, this view is shared by the organic chemistry community and, in fact, modern introductory texts to organic chemistry do not discuss "dative bonding", formulas with D→A bonds are nowhere to be found and covalent bonds dominate all Lewis–Kekulé structures.[63,64] In the absence of physically well defined population data, either approach provides a *formal* framework and, as purely *formal* representations, the notations D→A and

(59) Olah, G. A.; Grant, J. L. *J. Am. Chem. Soc.* **1975**, *97*, 1546.
(60) Korzeniowski, S. H.; Leopold, A.; Beadle, J. R.; Ahern, M. F.; Sheppard, W. A.; Khanna, R. K.; Gokel, G. W. *J. Org. Chem.* **1981**, *46*, 2153.
(61) (a) Schwartz, M. E. *J. Am. Chem. Soc.* **1972**, *94*, 6889. (b) Politzer, P.; Harris, R. R. *J. Am. Chem. Soc.* **1970**, *92*, 6451. (c) Politzer, P. *Theor. Chim. Acta* **1971**, *23*, 203. (d) Politzer, P.; Politzer, A. *J. Am. Chem. Soc.* **1973**, *95*, 5450.

(62) Cotton, F. A.; Wilkinson, G. *Advanced Inorganic Chemistry*, 5th ed.; Wiley & Sons, New York, 1988; p 35 ff.
(63) See for example: (a) McMurry, J. *Organic Chemistry*, 3rd ed.; Brooks/Cole Publ. Co., Pacific Grove, CA, 1992. (b) Carey, F. A. *Organic Chemistry*, 2nd ed.; McGraw-Hill, Inc.: New York, 1992. (c) Morrison, R. T.; Boyd, R. N. *Organic Chemistry*, 6th ed.; Prentice Hall, Englewood Cliffs, NJ, 1992. (c) Wade, L. G. *Organic Chemistry*, 2nd ed.; Prentice Hall: Englewood Cliffs, NJ, 1991. (d) Vollhardt, K. P. C.; Schore, N. E. *Organic Chemistry*, 2nd ed.; Freeman and Co.: New York, 1994 (dative bonds only are used to describe solvent coordination to Grignard reagents, p 258). (e) Fox, M. A.; Whitesell, J. K. *Organic Chemistry* Jones and Bartlett Publ.; Boston, MA, 1994. (f) Ege, S. *Organic Chemistry*, 3rd ed.; D. C. Heath & Co.: Lexington, MA, 1994. (g) Baker, A. D.; Engel, R. *Organic Chemistry*; West Publ. Co.: New York, 1992. (h) Fessenden, R. J.; Fessenden, J. S. *Organic Chemistry*, 5th ed.; Brooks/Cole Publ. Co.; Pacific Grove, CA, 1994. (i) Solomons, T. W. G. *Organic Chemistry*, 5th ed.; Wiley & Sons, Inc.: New York, 1992.
(64) There are very few exceptions. For example, Streitwieser, Heathcock, and Kosower describe a "coordinate covalent" bond or "coordinative" bond, but they also use this term for bookkeeping purposes only: Streitwieser, A.; Heathcock, C. H.; Kosower, E. M. *Introduction to Organic Chemistry*, 4th ed.; Macmillan Publ. Co.: New York, 1992; p 10, 162.

$D^+—A^-$ both have exactly the same logical validity.[65] The question is whether one should be satisfied with such a formalistic description of bonding. The answer has to be an unconditional "no". Consequently, a great number of proposals were put forth to distinguish between "covalent" and "dative" bonds and these have recently been reviewed.[66] Charge distributions are pivotal to discussions of bonding and reactivity, and every chemist should attempt to represent the electronic structure in a way that most closely reflects the physical reality of the molecular electron density distribution. With the advent of modern electron density analysis methods, it is possible to distinguish between the alternatives D→A and $D^+—A^-$ and it thus seems warranted and preferable to make the choice and select the physically more meaningful representation among the formally equivalent descriptions. On a purely formal level of classification, the descriptions of diazonium ions by the notations **I** or **II** are logically equivalent. However, our studies have shown that *the dative bond description* ***II*** *with an overall neutral* $N_2$ *group is clearly preferable* because it does more closely represent the actual electron density distribution in all kinds of diazonium ions. This distinction between "covalent" (**I**) and "dative" (**II**) bonding is made solely on the basis of the overall charge transfer determined with the *total* electron density distribution and without the knowledge of the molecules' reactivity and without reference to any other systems.[66b]

**Acknowledgment** is made to the donors of the Petroleum Research Fund, administered by the American Chemical Society, and to the University of Missouri—Columbia Research Board for support of this research. We thank Professors Heinrich Zollinger and Paul von Ragué Schleyer for many helpful discussions and suggestions. We thank the University of Missouri—Columbia Campus Computer Center for computer time and Dr. Ulrich Fleischer and Steve Meyer for their assistance with the IGLO installation.

JO951519U

(65) This very point is central to the discussion concerning the oxidation state and charge distributions in copper(III) complexes. (a) Snyder, J. P. *Angew. Chem., Int. Ed. Engl.* **1995**, *34*, 80. (b) Kaupp, M.; Schnering, H. G. v. *Angew. Chem., Int. Ed. Engl.* **1995**, *34*, 986. (c) Snyder, J. P. *Angew. Chem., Int. Ed. Engl.* **1995**, *34*, 986.

(66) (a) Haaland, A. *Angew. Chem., Int. Ed. Engl.* **1989**, *28*, 992 and references therein. (b) The C–N bonding in **1a** is "dative" in the sense of Haaland's energy condition; the minimum energy rupture of the C–N bond occurs indeed heterolytically, not homolytically. However, Haaland's discussion of cationic complexes is limited, and it is not clear whether his structural criteria can be generalized.